Interpretation of the hydrogen isotope effect on the density limit in JET-ILW L-mode plasmas using EDGE2D-EIRENE

V. Solokha[1], M. Groth[1], G. Corrigan[2], S. Wiesen[3] and JET contributors[*]

[1] *Aalto University, P.O. Box 14100, FI-00076, Aalto, Espoo, Finland*
[2] *EUROfusion Consortium, JET, Culham Science Centre, Abingdon, OX14 3DB, UK*
[3] *Forschungszentrum Jülich GmbH, Institut fur Energie- und Klimaforschung, IEK-4 - Plasmaphysik, 52425 Jülich, Germany*
[*] *See the author list of E. Joffrin et al. 2019 Nucl. Fusion 59 112021*

Corresponding author email: vladimir.solokha@aalto.fi

Abstract

Experiments in JET with the Be/W ITER-like wall show that in pure hydrogen low-confinement mode (L-mode) plasmas the density limit is approximately 20% higher than their corresponding deuterium plasmas. The maximum achievable density in L-mode plasmas is limited by the magnetohydrodynamic stability of the m/n=2/1 tearing mode.

EDGE2D-EIRENE studies show that the density of hydrogen atoms inside the separatrix is two times lower than for deuterium in plasma conditions preceding the density limit. The difference between isotopes is caused by the non-linear process at density limit onset, which leads to more efficient dissociation and ionization of hydrogen molecules and atoms in hydrogen than in deuterium plasmas at the inner X-point region at electron temperatures lower than 2 eV. The m/n=2/1 island size is estimated to be 30% smaller islands for hydrogen than for deuterium cases for equal fuelling conditions and radial transport assumptions.

1. Introduction

A tokamak-based fusion reactor heavily relies on high-density operation to satisfy the Lawson criterion with the least energy confinement time possible to become economically feasible. High-density operation increases the fusion output as $P_{fus} \propto n^2\langle\sigma v\rangle$ and at the same time

decreases the heat load on the divertor plates due to the transition to the detached regime [1]. The maximal achievable density in a tokamak is described by the Greenwald density limit scaling [2]. The Greenwald density scaling is describing the maximum reachable line-averaged density until magnetohydrodynamic (MHD) instabilities disrupt the discharge. The robust onset of the m/n=2/1 tearing mode [3] and a locked mode causes the plasma to contract and a disruption to be triggered by a thermal-resistive process [4].

Teng et al. [5] showed that the local power balance in the m/n=2/1 island can be used to predict the Greenwald density limit. In contrast to the power-independent Greenwald scaling, the density limit for JET L-mode plasmas in the case of the carbon wall and ITER-like wall (ILW) showed a dependence on total input power [6].

The isotope effect on the density limit (DL) in JET-C L-mode discharges has been investigated [7]. The conducted research showed that lighter hydrogen isotopes have higher density limits than heavier isotopes.

2. Experimental Observations

The isotope effect was investigated in JET-ILW ohmic discharges with plasma currents, I_P, of 2.0 MA, and on-axis toroidal magnetic field, B_T, of 2.0 T and ohmic heating, P_{ohm}, of approximately 2 MW, and in discharges with an additional NBI heating (I_P = 2.5 MA, B_T = 2.5 T, P_{ohm}+P_{NBI} = 4 MW). The configuration had the outer strike point on the horizontal part of the outer target and the ion $B \times \nabla B$ drift directed towards the divertor (favourable direction). The density was raised in linear fashion via the gas fuelling rate, I_{fuel}. Line-averaged density measurements in the

edge plasma were performed by the line-integrated interferometry diagnostic [8]. Two-dimensional poloidal distributions of radiated power were inferred from tomographic reconstructions of bolometer measurements [9]. The onset of the density limit included the increase in the radiated power accompanied by the consecutive plasma contraction visible in the interferometry data (Fig. 1). The time of the density limit (t_{DL}) is an estimation of the onset time in regard to the irreversible edge cooling. The locked mode amplitude peak is delayed by 0.1s from the DL, indicating the start of plasma mixing.

The DL of hydrogen pulses is 10-20% higher than the DL of deuterium pulses in ohmically heated cases, as well as in cases with additional NBI heating (table 1). At the same time, the power dependence of the DL is similar to the L-mode data from [6], as the doubled input power causes an approximately 50% increase in density limit.

At densities of $\langle n_e \rangle \approx 3 \cdot 10^{19}$m^{-3}, the neutral beam energy deposition profile shifts from the magnetic axis to the low-field side. As was shown by Rebut and Hugon [4], the power deficit inside the island causes the island growth. Therefore, in addition to ohmic power, NBI power sources tend to stabilize the island, allowing edge line-averaged density to reach $f_{GW} = 1.26$ in comparison to ohmic $f_{GW} = 0.95$, where f_{GW} is the Greenwald fraction ($f_{GW} = \langle n_e \rangle / n_{GW}$). The power balance of the island in pure hydrogen plasma can explain the observable dependence: $P_{ohm} + P_{ext} = n_e^2 L_H(T_e) \rightarrow n_e \propto \sqrt{P}$, where the $L_H = 5.35 \cdot 10^{-37} T_e^{1/2} (keV)\, W \cdot m^{-3}$ is the hydrogen cooling rate, the T_e is the electron temperature.

The H atoms have a higher velocity than D atoms at the same energy due to the mass difference, which affects the penetration profile and adds an isotope effect to the heating. To reduce the

complexity of the analysis, the pulses with additional heating were omitted. The analysis for NBI-heated pulses in JET-C can be found in [10].

Electron cyclotron emission (ECE) [11] measurements were used for measuring the electron temperature profiles with high temporal resolution. The T_e flattening near q=2 was observed 100 ms before the density limit.

The bolometer diagnostic captures the X-point radiation at the densities approximately 50% below the DL, as well as peak radiation movement to the high-field side before the disruption (Fig. 2). The total radiation losses at DL were equal for both isotopes at P_{rad} = 1.5 MW in L-mode pulses.

3. 2D SOL Simulations

The physics of the isotope effect on the density limit and the X-point radiation dynamics were investigated in the EDGE2D-EIRENE [12-14] simulations. The code utilized a magnetic configuration from JET pulse number 80295 representative of the experimental pure hydrogen and deuterium plasmas.

The fuelling ramp was simulated by a series of fixed gas fuelling simulations in the range from $I_{fuel} = 4.1 \cdot 10^{22} s^{-1}$ to $I_{fuel} = 5.0 \cdot 10^{22} s^{-1}$. The simulations were conducted without $E \times B$ and $B \times \nabla B$ drifts. Particle and heat diffusion coefficients were held constant for all fuelling rates and both isotopes identical to the values used in [15].

The EDGE2D-EIRENE simulations captured the movement of the radiation peak in the vicinity of the X-point to the high-field side. Potentially, the movement is mainly caused by the neutral particle leakage to the X-point from the inner target (IT) (Fig. 3). With increased fuelling, the molecular and atomic densities become sufficiently high to cool the plasma inside the separatrix to approximately 1-2 eV and to raise electron densities higher than $5 \cdot 10^{20}$ m^{-3}. Low T_e increases the ionisation mean free path for atoms and thus, effectively moves peak radiation inside the separatrix to the high-field side. The effective charge of the plasma remains equal to unity, thus the bremsstrahlung and impurity line radiation is negligible. The Ly-α emission dominates the radiation losses, contributing approximately 80% to the total radiated power. The radiation losses for H and D simulations at the DL onset are equal to P_{rad} = 1.1-1.2 MW, and the relative difference between isotopes is less than 8%.

At the DL onset, the atomic content in the confined plasma of the hydrogen cases is approximately a factor of 2 lower than in deuterium cases. In comparison, the pre-DL atomic content for the hydrogen is approximately 20-30% higher than for deuterium (Fig. 3).

Standalone EIRENE simulations on the same background plasma were executed to investigate the difference between the core penetration of atoms from the high-field and low-field sides of the X-point. The inward atomic-equivalent (H^0 + $2H_2$) current across the separatrix from the high-field side is 2 times larger than from the low-field side in H, whereas the difference for D simulations is about 6 times. Here, the atomic-equivalent current is defined as the inward current through the high- and low-field X-point surfaces. The inward current through both surfaces in

pre-DL conditions at the fuelling rate $I_{fuel} = 4.1 \cdot 10^{22} s^{-1}$ in the hydrogen case is 60% larger than for the deuterium case (Fig. 4). At a fuelling rate, of $I_{fuel} = 4.9 \cdot 10^{22} s^{-1}$, the inward hydrogen atomic-equivalent current through the high-field side X-point surface is 30% smaller than the deuterium atomic-equivalent current. The isotope effect on the inward current through the low-field X-point surface remains the same across the full range of fuelling rates.

In pre-DL conditions, hydrogen cases exhibit a 50% larger atomic-equivalent influx than deuterium cases due to the larger thermal velocity, and thus longer ionisation mean free path. The isotope effect on the inward atomic-equivalent current across the separatrix in pre-DL conditions, as well as, influx from the OT at DL limit onset is governed by the thermal velocity difference.

The inward hydrogen atomic-equivalent current from the IT at the DL onset is lower in hydrogen than in deuterium cases due to the non-linear interaction between plasma and neutral particles. The hydrogen cases have 50% lower molecular density near IT and X-point than deuterium, due to the higher thermal velocities [19]. Hypothetically, lower molecular densities lead to reduced local power losses by elastic scattering, thus higher T_e and better screening of atoms and molecules near separatrix in hydrogen cases compared to deuterium cases. As a consequence of the significantly larger deuterium atomic content in the confined region, the deuterium simulations demonstrate two times larger temperature reduction near the q=2 surface due to the Ly-α emission than the hydrogen simulations.

4. Tearing mode stability analysis

Analysis of the impact of the temperature reduction in the vicinity of q=2 surface on the m/n=2/1 tearing mode was done by utilizing the modified Rutherford equation (MRE) from the predictive model for the Greenwald density [5]. The MRE (Eq. 1) describes the island's growth:

$$(1) \quad \frac{dw}{dt} = 1.66\,\frac{\eta}{\mu_0}\,[\,\Delta'_{classic}(w) + \Delta'_{rad}(w) + \Delta'_{A}(w)]$$

where w is island width, η is the plasma resistivity, μ_0 is the magnetic permeability, $\boldsymbol{\Delta'}_{\text{classic}}$ is the classical term (Eq. 2) approximated in [16], the $\boldsymbol{\Delta'}_{\text{rad}}$ (Eq. 3) is the current perturbation term caused by radiation-induced cooling, the $\boldsymbol{\Delta'}_{\text{A}}$ (Eq. 4) is the island asymmetry term. The latter two terms were derived in [17] as

$$(2) \quad \Delta'_{classic}(w) = 2\,\frac{r_s}{a}\left(1 - 23\,\frac{w}{a}\right)$$

$$(3) \quad \Delta'_{rad}(w) = \frac{16\,\mu_0\langle\delta j_1\rangle}{\psi''_0(r_s)}\,\frac{w}{w^2+w_F^2}$$

$$(4) \quad \Delta'_{A}(w) = \frac{16\,\mu_0 j'_o(r_x)}{\pi\psi''_0(r_s)}\,\frac{w^2}{w^2+w_F^2}A_s f_F$$

where $\langle\delta j_1\rangle$ is the current perturbation estimated from the temperature reduction caused by radiation, ψ''_0 is the second derivative of the zeroth-order helical flux at the rational surface, j'_o is the first derivative of the current density, w_F is the Fitzpatrick critical island width, r_x is the location of the island X-point, r_s is the location of the resonant surface, A_s is the island asymmetry, f_F is the Fitzpatrick factor and a is the plasma minor radius. The sole term which includes the isotope effect, due to the difference in core penetration of the atoms, is the radiative term $\boldsymbol{\Delta'}_{\text{rad}}$. Thus, the classic and the asymmetry terms are identical for hydrogen and deuterium. The w_F, A_s and f_F were assumed to be equal to 0.05 m, 1.5, and 1.0, correspondingly.

The impact of temperature reduction on the current density is described by the conductivity

dependent on T_e [17]. In this case, the temperature difference is assumed to be caused by the atoms penetrating from the divertor, and T_e at the q=2 flux surface was estimated by the EDGE2D-EIRENE simulations.

The island width in deuterium plasmas is predicted to be larger than in hydrogen plasmas (Fig. 5). As the deuterium simulations predict a larger T_e reduction described in the previous section, the island growth rate caused by the current perturbation due to the radiative cooling of the plasma will be higher as all of the other terms stay the same. At the fuelling rate of, $I_{fuel} = 4.5 \cdot 10^{22} s^{-1}$ the difference between the isotopes is negligible. When the fuelling increases up to $I_{fuel} = 5.0 \cdot 10^{22} s^{-1}$ the difference becomes approximately 30%. The hydrogen plasmas will reach the critical island size at a higher fuelling rate than deuterium pulses, and therefore one can be expected to achieve higher densities.

5. Discussion

The ohmic power dependency on the volume-averaged density was included in dedicated simulations. The decreasing temperature causes a rise in the plasma resistivity and therefore a 10% increase in ohmic power is observed during the fuelling ramp. The EDGE2D-EIRENE simulations with the input power as a function of the fuelling/recycling rate exhibited the same behaviour in terms of the isotope effect, while the code-predicted DL was higher for both isotopes.

Further extrapolation of the simulation results to tritium was not accomplished at the writing of

the manuscript. Tritium plasmas are expected to have lower DL than deuterium. EDGE2D-EIRENE simulations of the tritium plasmas were conducted in the pulse 80295 configuration with hydrogen atomic and molecular reactions cross-sections. The results presented in this paper imply 50% higher tritium atomic density inside the confined region at a fuelling rate of $I_{fuel} = 4.8 \cdot 10^{22} s^{-1}$ compared to the deuterium case. Thus, a monotonic dependency of the isotope effect on the DL is suggested by these studies, while the additional tritium experiments are expected to verify the discussed predictions.

6. Conclusions

The impact of the isotope species on the DL in JET-ILW was investigated experimentally and interpreted by means of EDGE2D-EIRENE simulations. The thermo-resistive DL model was successfully used to explain the observed difference in DL between hydrogen and deuterium JET-ILW L-mode plasmas. Hydrogen plasmas showed 10-20% higher DL than deuterium pulses at equal total radiation within the entire plasma of P_{rad} = 1.5 MW in experiments.

At the onset of the density limit, EDGE2D-EIRENE simulations predict $T_e < 2$ eV across the confined plasma region. At these temperatures, the influx of hydrogen atoms is 30% lower than that of deuterium, presumably due to the 50% lower molecular densities in hydrogen cases than in deuterium cases. The position of the Ly-α radiation peak for hydrogen cases is further away from the q=2 surface than for deuterium cases. The cold plasma around the q=2 surface is prone to the m/n=2/1 tearing mode destabilisation and in DL conditions the typical island size for hydrogen is 1.4 times smaller than for deuterium. Both effects result in discharge termination for lighter isotopes to occur at higher line-averaged densities than for

heavy isotopes.

Acknowledgements

This work has been carried out within the framework of the EUROfusion Consortium and has received funding from the Euratom research and training programme 2014-2018 and 2019-2020 under grant agreement No 633053. The views and opinions expressed herein do not necessarily reflect those of the European Commission. The authors are grateful to G. Pucella and A. Holm for useful discussions.

References

[1] R. A. Pitts, et al. (2019) Nuclear Materials and Energy 20 100696
https://doi.org/10.1016/j.nme.2019.100696

[2] M. Greenwald (2002) Plasma Phys. Control. Fusion 44 R27
https://doi.org/10.1088/0741-3335/44/8/201

[3] W. Suttrop, et al., 1997 Nucl. Fusion 37 119
https://doi.org/10.1088/0029-5515/37/1/I09

[4] P. Rebut and M. Hugon (1984), Plasma Physics and Controlled Nuclear Fusion Research, vol. 2 (Vienna: IAEA) p. 197
http://www-naweb.iaea.org/napc/physics/FEC/STIPUB670_VOL2.pdf

[5] Q. Teng, et al., (2016) Nucl. Fusion 56 106001
http://dx.doi.org/10.1088/0029-5515/56/10/106001

[6] A. Huber, et al., (2013) Journal of Nuclear Materials, 438, S139-S147

https://doi.org/10.1016/j.jnucmat.2013.01.022

[7] C.F. Maggi, et al., (1999) Nucl. Fusion 39 979

https://doi.org/10.1088/0029-5515/39/8/303

[8] G. Braithwaite, et al., (1989) Review of Scientific Instruments 60, 2825

https://doi.org/10.1063/1.1140666

[9] A. Huber, et al., (2007) Fusion Engineering and Design, 82, 5–14, 1327-1334

https://doi.org/10.1016/j.fusengdes.2007.03.027

[10] K. Borrass, et al., (1997) Nucl. Fusion 37 523

https://doi.org/10.1088/0029-5515/37/4/I10

[11] E. de la Luna, et al., (2004) Review of Scientific Instruments 75, 3831

https://doi.org/10.1063/1.1781376

[12] R. Simonini, et al., (1994) Contrib. Plasma Phys. 34 368–373,

https://doi.org/ 10.1002/ctpp.2150340242

[13] S. Wiesen et al., (2006) JET ITC-Report

http://eirene.de/e2deir_report_30jun06.pdf

[14] D. Reiter, M. Baelmans, P. Borner, (2005) Fusion Sci. Technol. 47 172–186,

https://doi.org/10.13182/FST47-172.

[15] V. Solokha et al., (2020) Nuclear Materials and Energy, 25, 100836

https://doi.org/10.1016/j.nme.2020.100836

[16] Q. Yu, et al., (2004) Phys. Plasmas 11, 1960 ;

https://doi.org/10.1063/1.1710521

[17] R.B. White, D.A. Gates and D.P. Brennan (2015) Phys. Plasmas

22 022514; http://dx.doi.org/10.1063/1.4913433

Tables

Table 1:

	P_{ohm} (2 MW)	P_{ohm} (2 MW) + P_{NBI} (2 MW)
$\langle n^{DL}_{H} \rangle$, m^{-3} (f_{GW})	$3.8 \cdot 10^{19}\, m^{-3}$ (0.95)	$6.3 \cdot 10^{19}\, m^{-3}$ (1.26)
$\langle n^{DL}_{D} \rangle$, m^{-3} (f_{GW})	$3.2 \cdot 10^{19}\, m^{-3}$ (0.80)	$4.8 \cdot 10^{19}\, m^{-3}$ (0.96)

Table captions:

Table 1:

The density limit and Greenwald fraction for hydrogen and deuterium plasmas in ohmically heated pulses 87640 (H) and 80331 (D), I_P = 2 MA, B_T = 2 T, P_{OH} = 2 MW; externally heated pulses 91278 (H) and 90415 (D), I_P = 2.5 MA, B_T = 2.5 T, P_{OH+NBI} = 4 MW.

Figures

Figure 1:

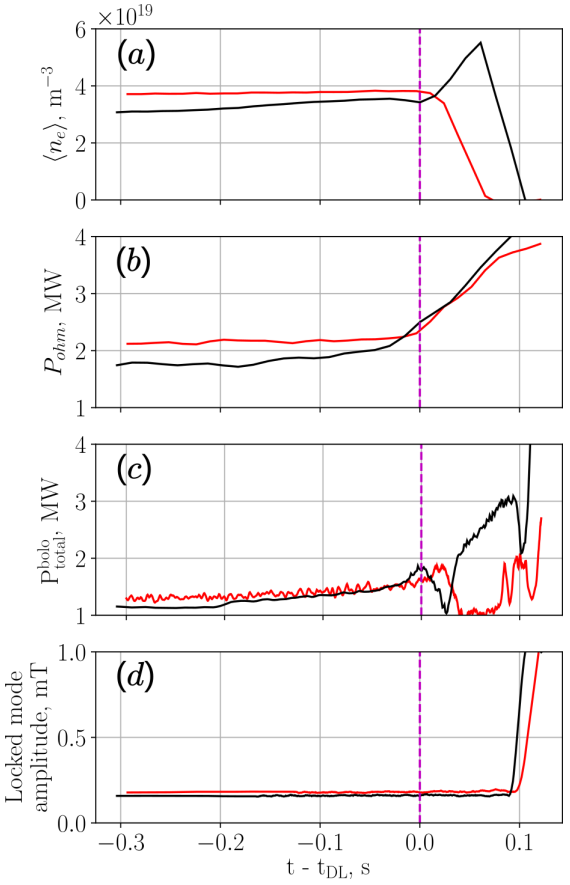

Figure 2:

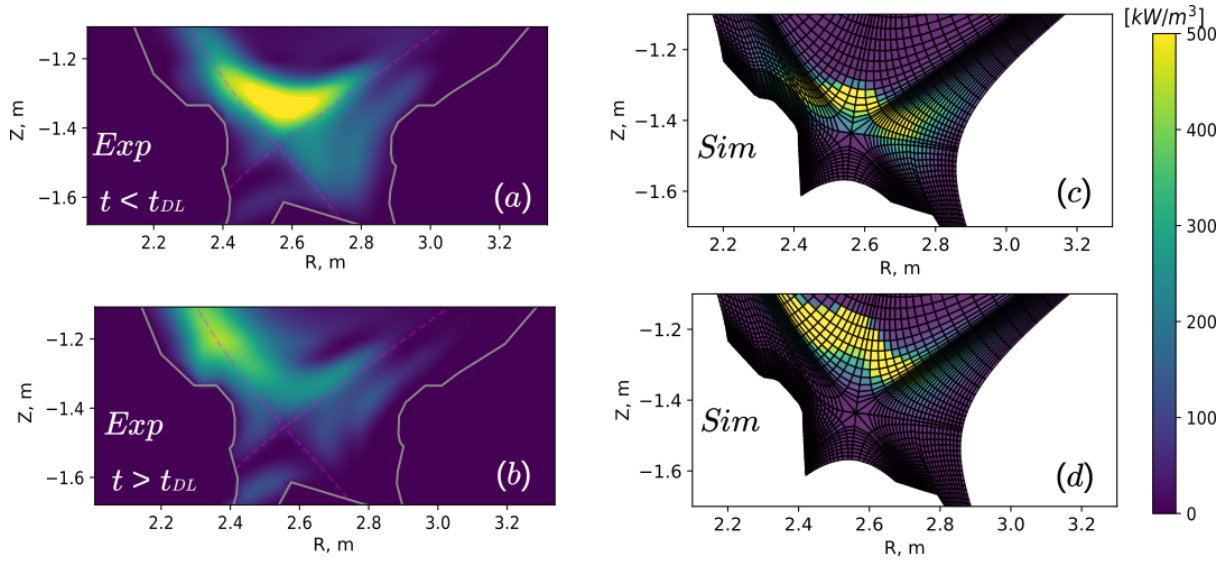
Exp
$t < t_{DL}$
(a)
Exp
$t > t_{DL}$
(b)
Sim
(c)
Sim
(d)
Z, m
R, m
−1.2
−1.4
−1.6
2.2
2.4
2.6
2.8
3.0
3.2
$[kW/m^3]$
500
400
300
200
100
0

Figure 3:

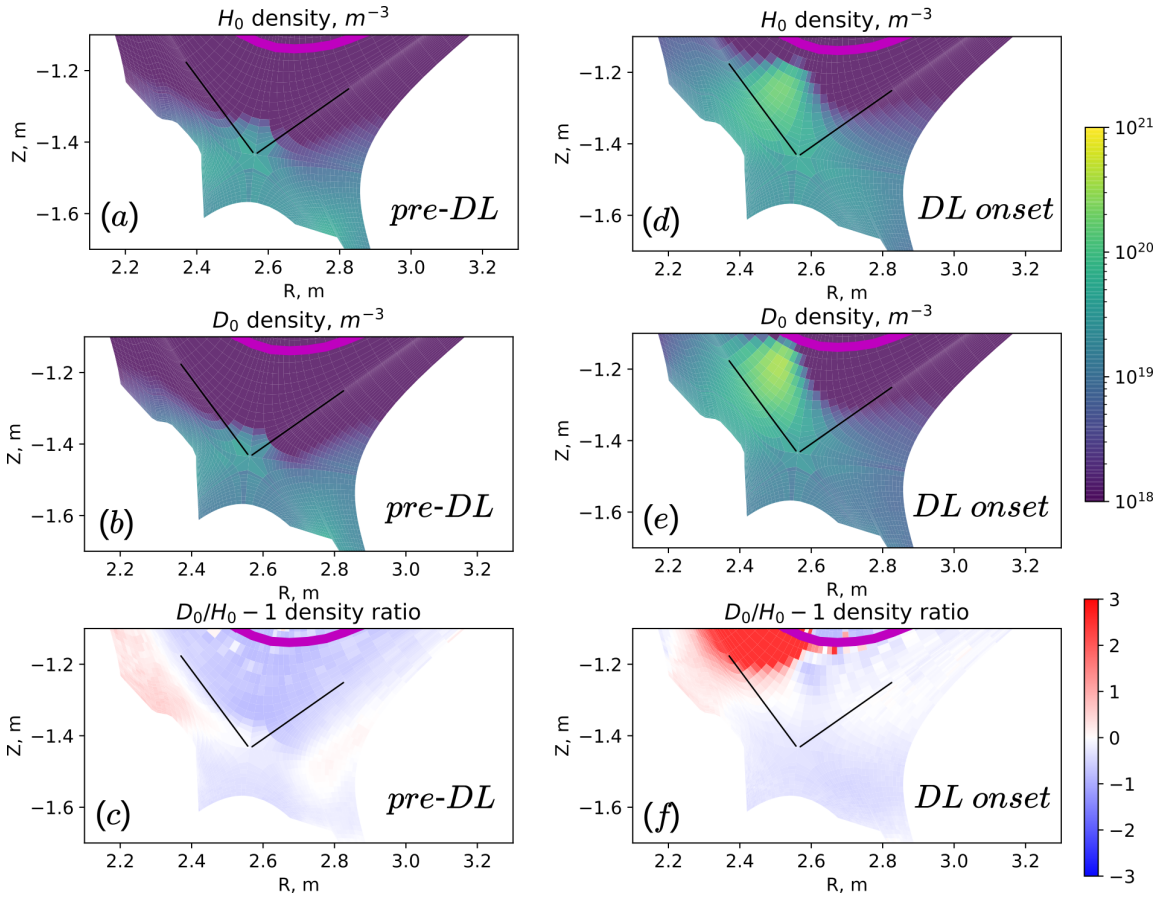
H_0 density, m^{-3}
D_0 density, m^{-3}
$D_0/H_0 - 1$ density ratio
Z, m
R, m
(a)
(b)
(c)
(d)
(e)
(f)
pre-DL
DL onset
10^{21}
10^{20}
10^{19}
10^{18}

Figure 4:

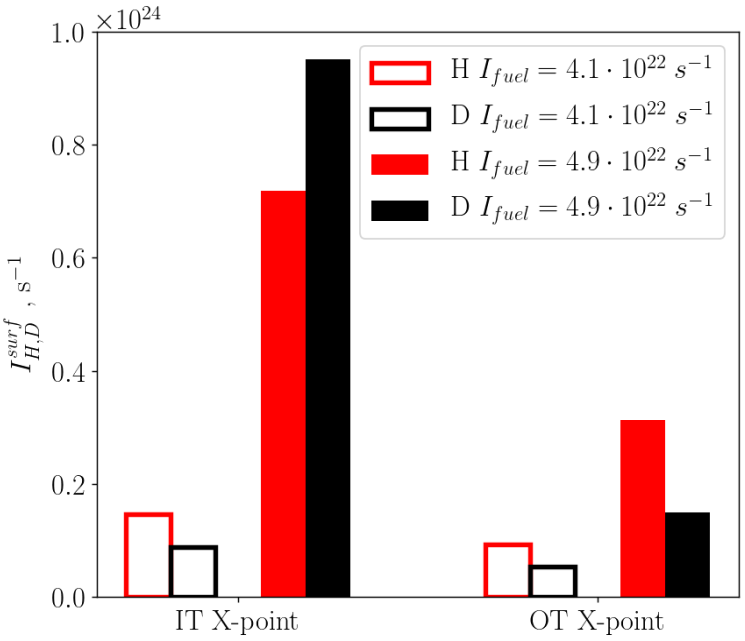

Figure 5:

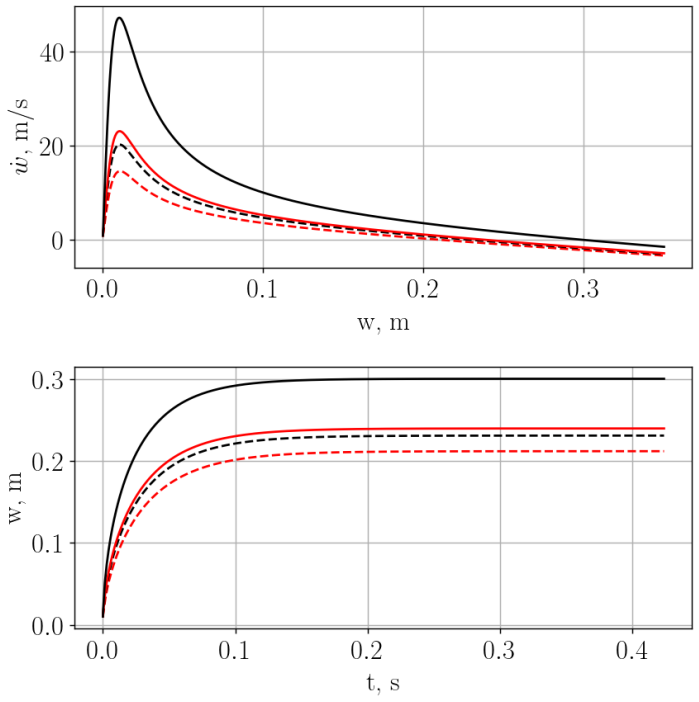

Figure captions:

Figure 1:

(a) Line-averaged density, (b) ohmic power, (c) total radiated power and (d) locked mode amplitude for hydrogen pulse 87640 (red) and deuterium pulse 80331 (black). The vertical magenta line is the approximate density limit onset time.

Figure 2:

2D bolometry reconstruction data from hydrogen pulse 87640, 20 ms before the DL (a) and during the plasma contraction (b).

The EDGE2D-EIRENE simulation of radiative losses in hydrogen cases with fuelling rates $I_{fuel} = 4.3 \cdot 10^{22} s^{-1}$(c) and $I_{fuel} = 5.0 \cdot 10^{22} s^{-1}$(d).

Figure 3:

2D distribution of atomic density for hydrogen (a) and deuterium (b) cases with fuelling rate $I_{fuel} = 4.1 \cdot 10^{22} s^{-1}$with the density ratio - 1 shown in (c), and for hydrogen (d) and deuterium (e) cases with fuelling rates $I_{fuel} = 5.0 \cdot 10^{22} s^{-1}$ with density ratio - 1 shown in (f). Black lines indicate positions of diagnostic surfaces.

Figure 4:

Atomic-equivalent inward current through diagnostic surfaces for hydrogen (red) and deuterium (black) cases with $I_{fuel} = 4.1 \cdot 10^{22} s^{-1}$ (hollow bars) and $I_{fuel} = 4.9 \cdot 10^{22} s^{-1}$ (filled bars).

Figure 5:

Island growth rates (top) and island size (bottom) for hydrogen (red) and deuterium (black) cases with $I_{fuel} = 4.5 \cdot 10^{22} s^{-1}$ (dashed) and $I_{fuel} = 5.0 \cdot 10^{22} s^{-1}$(solid).